ETH
Eidgenössische Technische Hochschule Zürich
Swiss Federal Institute of Technology Zurich

Seminar for Applied Mathematics SAM

Well-balanced schemes for gravitationally stratified media

R. Käppeli and S. Mishra

Research Report No. 2014-37
December 2014

Seminar für Angewandte Mathematik
Eidgenössische Technische Hochschule
CH-8092 Zürich
Switzerland

Volume Title
ASP Conference Series, Vol. **Volume Number**
Author

Well-balanced schemes for gravitationally stratified media

Roger Käppeli and Siddhartha Mishra

Seminar for Applied Mathematics (SAM), Department of Mathematics, ETH Zürich, CH-8092 Zürich, Switzerland

Abstract. We present a well-balanced scheme for the Euler equations with gravitation. The scheme is capable of maintaining exactly (up to machine precision) a discrete hydrostatic equilibrium without any assumption on a thermodynamic variable such as specific entropy or temperature. The well-balanced scheme is based on a local hydrostatic pressure reconstruction. Moreover, it is computationally efficient and can be incorporated into any existing algorithm in a straightforward manner. The presented scheme improves over standard ones especially when flows close to a hydrostatic equilibrium have to be simulated. The performance of the well-balanced scheme is demonstrated on an astrophysically relevant application: a toy model for core-collapse supernovae.

1. Introduction

In many interesting astrophysical phenomena the flow is close to hydrostatic equilibrium

$$\nabla p = -\rho \nabla \phi. \tag{1}$$

This is for instance the case when simulating wave propagation in stellar atmospheres, convection in stellar interiors and the climate of exoplanets. In these examples, hydrostatic equilibrium dominates and the flow of interest is realized as a perturbation of it. In other situations, hydrostatic equilibrium may be dominating only in a certain region, whereas in other regions the flow may be fully dynamic. Moreover, the region close to equilibrium may be the result of a dynamic process. This is for example the case in the core-collapse supernova scenario, where the collapse of the core of an evolved massive star results in the formation of a highly compact massive object. This object, which is to become a neutron star [1], is very close to hydrostatic equilibrium. However, the fate of the supernova explosion is sealed just above this proto-neutron star in a very dynamic environment.

In the situations mentioned above, the interest relies in robust and accurate numerical resolution of flows close to hydrostatic equilibrium. The numerical approximation of near steady flows is challenging for standard finite volume schemes as they do not necessarily satisfy a discrete equivalent of the balance of pressure gradient and gravitational forces. As a result, equilibrium states are not preserved exactly but are approximated with an error proportional to the truncation error. So if one is interested in the

[1] We focus here on events leaving behind a neutron star.

simulation of the particular types above, the numerical resolution has to be increased to the point that the truncation errors do not obscure the phenomena of interest. This need in resolution may become prohibitively large (especially in multiple dimensions).

To overcome this challenge, we seek a scheme that satisfies a discrete version of the delicate balance (1). Schemes having such a property have been coined as well-balanced. However, the equilibrium eq. (1) only specifies a mechanical equilibrium. Käppeli & Mishra (2014) have designed a well-balanced scheme under the further assumption of a thermal equilibrium. By assuming isentropic (isothermal) conditions, eq. (1) can be explicitly integrated to $h + \phi = const.$ ($g + \phi = const.$), where h is the specific enthalpy (g the Gibbs free energy). These expressions can then be used to build a well-balanced scheme for the isentropic (isothermal) case. However, the assumption on a thermal equilibrium is not adequate in all instances. Especially when the equilibrium is the outcome of a dynamic process.

In this contribution, we shall present a well-balanced scheme that does not rely on any assumption of a thermal equilibrium. A mechanical equilibrium is directly built from a discrete version of (1). In section 2 we shall derive the well-balanced scheme and its use is illustrated at a toy model of core-collapse supernova explosions in 3. More extensive presentations and examples will be presented in a forthcoming publication.

2. Well-balanced scheme

2.1. One-dimensional Cartesian

In one space dimension the Euler eqs. can be recast in the following compact form

$$\frac{\partial \mathbf{u}}{\partial t} + \frac{\partial \mathbf{F}}{\partial x} = \mathbf{S} \tag{2}$$

with

$$\mathbf{u} = \begin{bmatrix} \rho \\ \rho v_x \\ E \end{bmatrix}, \quad \mathbf{F} = \begin{bmatrix} \rho v_x \\ \rho v_x^2 + p \\ (E + p) v_x \end{bmatrix} \quad \text{and} \quad \mathbf{S} = - \begin{bmatrix} 0 \\ \rho \\ \rho v_x \end{bmatrix} \frac{\partial \phi}{\partial x}, \tag{3}$$

where $\mathbf{u}$, $\mathbf{F}$ and $\mathbf{S}$ are the vectors of conserved variables, fluxes and source terms. We will denote the primitive variables by $\mathbf{w} = [\rho, v_x, p]^T$.

Finite volume schemes compute numerical approximations to solutions of conservation laws by discretizing space into finite volumes or cells $I_i = [x_{i-1/2}, x_{i+1/2}]$ of regular size $\Delta x = x_{i+1/2} - x_{i-1/2}$ (for simplicity of the presentation). Cell centers are given by $x_i = (x_{i-1/2} + x_{i+1/2})/2$. By integrating eq. (2) over a cell I_i one obtains a semi-discrete finite volume scheme for the evolution of the cell averaged conserved variables

$$\frac{\mathrm{d}\mathbf{u}_i}{\mathrm{d}t} = -\frac{1}{\Delta x} \left(\mathbf{F}_{i+1/2} - \mathbf{F}_{i-1/2} \right) + \mathbf{S}_i, \tag{4}$$

where $\mathbf{F}_{i+1/2}$ is the numerical flux at cell interface and $\mathbf{S}_i$ is the cell averaged gravity source term.

The numerical flux is obtained by solving (approximately) the Riemann problem at cell interfaces

$$\mathbf{F}_{i+1/2} = \mathcal{F}(\mathbf{w}_{i+1/2-}, \mathbf{w}_{i+1/2+}), \tag{5}$$

where the $\mathbf{w}_{i+1/2-}$ and $\mathbf{w}_{i+1/2+}$ denote the cell interface extrapolated primitive variables. For the well-balanced scheme elaborated below we require that the numerical flux is capable of resolving stationary contact discontinuities, i.e.

$$\mathcal{F}\left([\rho_L, 0, p]^T, [\rho_R, 0, p]^T\right) = [0, p, 0]^T, \tag{6}$$

where ρ_L (ρ_R) is the density on the left (right) side of the contact discontinuity and p the constant pressure. For example the HLLC (Toro et al. 1994) and Roe (Roe 1981) approximate Riemann solvers have this property. In the numerical example presented below, we have used the HLLC Riemann solver with wave speed estimates according to Batten et al. (1997).

The gravitational source term is evaluated by standard second-order central differences

$$\mathbf{S}_i = -\begin{bmatrix} 0 \\ \rho_i \\ (\rho v_x)_i \end{bmatrix} \frac{\phi_{i+1} - \phi_{i-1}}{2\Delta x}, \tag{7}$$

where the ϕ_i are the cell centered values of the gravitational potential.

The cell interface extrapolated variables are obtained by reconstruction from the cell averages. Commonly, some non-oscillatory piece-wise polynomial reconstruction of the TVD, ENO or WENO type is used (see e.g. Toro (1997) and references therein). However, these reconstructions are not well suited for the case of interest here. The reason for this is simply the fact that a hydrostatic equilibrium is generally not a piece-wise polynomial function. In the following subsection, we build a reconstruction that automatically fulfills a discrete version of hydrostatic equilibrium (without any assumption on a thermal equilibrium).

2.2. Well-balanced pressure reconstruction

In hydrostatic equilibrium, gravity forces are exactly balanced by the pressure gradient force

$$\frac{\partial p}{\partial x} = -\rho \frac{\partial \phi}{\partial x}. \tag{8}$$

This subtle balances is not readily maintained by standard schemes based on non-oscillatory polynomial reconstruction.

In the first-order scheme, we propose to reconstruct the cell interface primitive variables by

$$\mathbf{w}_{i\mp 1/2\pm} = \begin{bmatrix} \rho_i \\ v_{x,i} \\ p_{i\mp 1/2\pm} \end{bmatrix}, \tag{9}$$

i.e. a piece-wise constant reconstruction of density and velocity, and for the pressure

$$p_{i-1/2+} = p_i + \rho_i \frac{\phi_i - \phi_{i-1}}{\Delta x} \frac{\Delta x}{2} \quad \text{and} \quad p_{i+1/2-} = p_i - \rho_i \frac{\phi_{i+1} - \phi_i}{\Delta x} \frac{\Delta x}{2}. \tag{10}$$

This pressure reconstruction takes explicitly into account the pressure variation induced by gravity. Moreover, it is consistent with the central discretization of the momentum component of the gravitational source term eq. (7), i.e.

$$\frac{p_{i+1/2-} - p_{i-1/2+}}{\Delta x} = -\rho_i^n \frac{\phi_{i+1} - \phi_{i-1}}{2\Delta x}. \tag{11}$$

In hydrostatic equilibrium the pressure is continuous everywhere. Now consider the $i + 1/2$-th cell interface. If the reconstructed pressure from cell i and $i + 1$ are in equilibrium at this interface, i.e. $p_{i+1/2-} = p_{i+1/2+}$, the following holds:

$$\frac{p_{i+1} - p_i}{\Delta x} = -\frac{\rho_i + \rho_{i+1}}{2} \frac{\phi_{i+1} - \phi_i}{\Delta x}, \tag{12}$$

which is clearly a (spatially) second-order accurate discretization of hydrostatic equilibrium (8). Moreover, this is the discrete hydrostatic equilibrium that is exactly preserved by our reconstruction.

2.3. The well-balanced scheme and its extensions

A well-balanced semi-discrete finite volume scheme can then be assembled by combining the hydrostatic reconstruction (9), a contact discontinuity resolving Riemann solver (5) and the semi-discrete evolution prescription (4) for the conserved variables.

Now, suppose we are given a discrete pressure p_i, density ρ_i and gravitational potential ϕ_i profile fulfilling eq. (12) and vanishing velocity $v_i = 0$. Then, this discrete hydrostatic equilibrium is preserved exactly (or up to machine precision) by our well-balanced scheme:

$$\frac{\mathrm{d}\mathbf{u}_i}{\mathrm{d}t} = 0. \tag{13}$$

Therefore, we have built a well-balanced hydrostatic equilibrium preserving scheme without any assumption on a thermodynamic variable such as specific entropy or temperature. This is a substantial improvement over Käppeli & Mishra (2014), where isentropic or isothermal conditions had to be assumed.

Although the hydrostatic equilibrium preserved by the scheme is (spatially) second-order accurate, any perturbation on top of this stationary state is only resolved with first-order accuracy. In a similar manner as Käppeli & Mishra (2014), a second-order well-balanced pressure reconstruction can be built by applying a piece-wise linear reconstruction to the equilibrium perturbation. For the density and the velocity a standard piece-wise linear reconstruction can be applied. In the numerical tests below, we have used a MUSCL type piece-wise linear reconstruction with the monotonized centered limiter.

The well-balanced scheme can also be generalized to different geometries (cylindrical and spherical) and higher dimensions. The multidimensional generalization can be achieved in a direction-by-direction manner.

3. Application: a toy model of core-collapse

As an illustration of the performance of our well-balanced scheme, we apply it to a toy model of core-collapse supernovae from Janka et al. (1993). This example simulates in spherical symmetry the collapse, bounce, evolution of the induced shock waves and formation of a proto-neutron (PNS) for a simplified model of a stellar core and equation of state. The forming PNS is close to hydrostatic equilibrium. Because the PNS is the outcome of a very dynamic process, it is interesting to investigate how accurately the well-balanced scheme captures the near equilibrium state.

The initial configuration models the iron core of an evolved massive star. It consists of an equilibrium polytrope with polytropic index $n = 3$ (corresponding to an

adiabatic index $\gamma = 4/3$), polytropic constant $K = 4.897 \times 10^{14}$ (in cgs units) and a central density $\rho_c = 10^{10}$ g/cm^3. This corresponds to a total mass $M \approx 1.44 M_\odot$ and a radius $R \approx 1.54 \times 10^3$ km.

The EoS consists of a purely polytropic part and a thermal part. The polytropic part is chosen to mimic the behavior of a relativistic and degenerate electron gas at low densities $\rho < 2 \times 10^{14}$ g/cm^3. At higher densities, it mimics the stiffening of a nuclear gas EoS above nuclear saturation density. See Janka et al. (1993) for further details.

The polytrope is then set up on a radial domain $[0, 1.5 \times 10^3]$ km and discretized by $N = 128, 256, 512, 1024, 8192$ zones with an exponentially growing size $\Delta r_i = a^{i-1} \Delta r_1$, $i = 2, ..., N$. Here $a \geq 1$ is the grid scaling parameter and Δr_1 the size of the first zone. For the resolutions we have taken $\Delta r_1 = 2, 1, 0.5, 0.25, 0.025$ km, respectively. The finest resolution serves as a reference solution.

The polytrope is then evolved with a standard and the well-balanced schemes for all resolutions from $t = 0$ up to 110 ms. The collapse is initiated by slightly lowering the adiabatic exponent from 4/3 to 1.325. The collapse goes on until the central density exceeds 2×10^{14} g/cm^3, where the EoS stiffens. This allows the inner-core, the inner part that collapses subsonically, to progressively halt the collapse and, eventually, to find a new equilibrium configuration, i.e. the "toy" PNS is born. Starting at the center of the inner core, where the density is largest, successive mass shells are stopped. Pressure waves move out in radius and accumulate near the sonic point, i.e. the point where the collapse velocity equals the speed of sound, where they steepen into a shock wave. Due to its inertia, the inner core overshoots its equilibrium and rebounds behind the shock wave: the core bounces.

In this simple model for core-collapse, the energy transferred to the shock wave is large enough to make the polytrope explode, leaving behind a highly compact object (the "toy" PNS). It's now interesting to compare the performance of the standard and the well-balanced scheme in the numerical resolution of the PNS. The well-balanced scheme consists of the pressure reconstruction outlined in section 2 with its second-order extension and time is integrated by the Heun method. In the standard scheme, a standard piece-wise linear reconstruction is used for all variables.

A measure on how well a numerical scheme is able to resolve the near equilibrium of the PNS is given by the evolution of the central density, which should remain roughly constant (after post-bounce oscillations have stopped). In figure 1 we plot the central density as a function of time for the standard and the well-balanced scheme for different resolutions. From the figure it is clear, that the standard scheme has troubles for $N < 512$. Even at $N = 512$ one can discern a drift in the central density. On the contrary, the well-balanced scheme is able to maintain the nearly constant central density at all resolutions (with a slight overestimate for $N = 128$).

In figure 2 we show the integrated total internal, kinetic and gravitational energies as a function of time for both schemes with $N = 512$. Also the error in total energy conservation is displayed. After bounce, we observe that the standard scheme shows a steadily growing error in total energy conservation. The reason behind this steadily growing error is that it's not able (at the present resolution) to maintain the PNSs hydrostatic equilibrium. As a matter of fact, the overwhelming majority of integrated internal and gravitational energy is enclosed in the PNS. On the other hand, the well-balanced scheme shows a constant error in energy conservation after bounce simply because it's able to resolve the hydrostatic equilibrium much better.

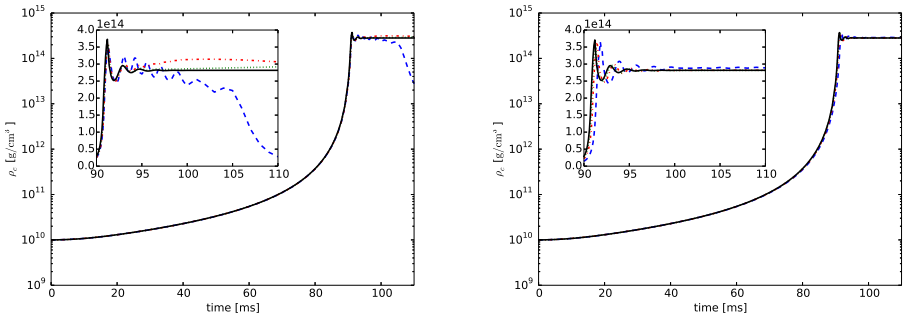

Figure 1. Central density as a function of time for the standard (left panel) and the well-balanced (right panel) schemes. In both panels the dashed (blue), dash-dotted (red), dotted (green) and the solid (black) line represent the simulations with $N = 128, 256, 512, 8192$, respectively.

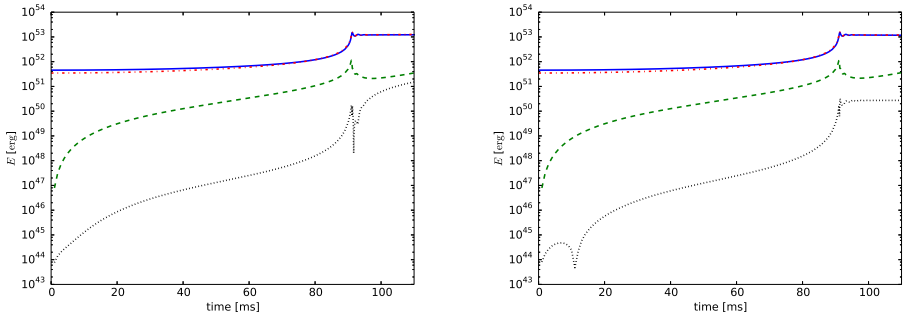

Figure 2. Energies and total energy conservation as a function of time for the standard (left panel) and well-balanced (right panel) schemes with $N = 512$. In both panels the solid (blue) line is the total internal energy, the dashed (green) line is the total kinetic energy, the dash-dotted (red) line is minus the total gravitational energy and the dotted (black) line is the total energy conservation.

4. Conclusion

We have presented a well-balanced scheme for hydrostatic equilibrium. We have shown that the scheme substantially improves upon standard ones at the example of a toy model for core-collapse. A more comprehensive description of the well-balanced scheme as well as more astrophysically relevant applications will be exposed in a forthcoming publication.

References

Batten, P., Clarke, N., Lambert, C., & Causon, D. M. 1997, SISC, 18, 1553
Janka, H.-T., Zwerger, T., & Moenchmeyer, R. 1993, A&A, 268, 360
Käppeli, R., & Mishra, S. 2014, JCP, 259, 199
Roe, P. L. 1981, JCP, 43, 357
Toro, E. F. 1997, Riemann Solvers and Numerical Methods for Fluid Dynamics (Springer)
Toro, E. F., Spruce, M., & Speares, W. 1994, Shock Waves, 4, 25

Recent Research Reports

Nr.	Authors/Title

2014-27 R. Hiptmair and A. Paganini
Shape optimization by pursuing diffeomorphisms

2014-28 D. Ray and P. Chandrashekar and U. Fjordholm and S. Mishra
Entropy stable schemes on two-dimensional unstructured grids

2014-29 H. Rauhut and Ch. Schwab
Compressive sensing Petrov-Galerkin approximation of high-dimensional parametric operator equations

2014-30 M. Hansen
A new embedding result for Kondratiev spaces and application to adaptive approximation of elliptic PDEs

2014-31 F. Mueller and Ch. Schwab
Finite elements with mesh refinement for elastic wave propagation in polygons

2014-32 R. Casagrande and C. Winkelmann and R. Hiptmair and J. Ostrowski
DG Treatment of Non-Conforming Interfaces in 3D Curl-Curl Problems

2014-33 U. Fjordholm and R. Kappeli and S. Mishra and E. Tadmor
Construction of approximate entropy measure valued solutions for systems of conservation laws.

2014-34 S. Lanthaler and S. Mishra
Computation of measure valued solutions for the incompressible Euler equations.

2014-35 P. Grohs and A. Obermeier
Ridgelet Methods for Linear Transport Equations

2014-36 P. Chen and Ch. Schwab
Sparse-Grid, Reduced-Basis Bayesian Inversion